

Oxygen-promoted hydrogen adsorption on activated and hybrid carbon materials

S. Schaefer^a, A. Jeder^{a,b}, G. Sdanghi^{a,d}, P. Gadonneix^a, A. Abdedayem^b, M.T Izquierdo^c, G. Maranzana^d, A. Ouederni^b, A Celzard^a, V. Fierro^{a,*}

Supplementary information

Table S1: Elemental composition from EA and XPS.

Element Materials	Elemental Analysis (EA)					XPS Analysis			
	C wt. %	H wt. %	O wt. %	N wt. %	S wt. %	C at. %	O at. %	N at. %	K at. %
180_KOH_W	71.8	3.2	19.1	0.2	0.0	80.1	17.6	0.3	1.9
180_KOH_UW	51.6	3.4	29.6	0.1	0.3	52.4	41.5	0.3	5.7
240_KOH_UW	54.3	3.2	26.6	0.2	0.0	67.7	26.3	0.1	5.9
180_KOH_W_O3	80.2	4.6	14.6	0.3	0.3	77.2	22.5	0.3	0.0
240_KOH_W_O3	75.3	3.6	20.6	0.3	0.0	76.6	23.0	0.2	0.2
CO2_2h	87.9	2.4	7.5	2.2	0.0	86.7	12.8	0.5	0.0

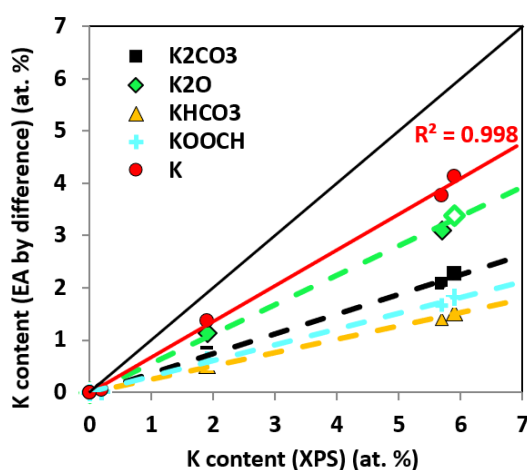


Figure S1: Comparison between the potassium contents obtained by XPS and EA for different K-containing structures.

Table S2: Corrected elemental composition using different model compounds (from EA).

K₂CO₃		Elemental Analysis (EA)					
Element	C at. %	H at. %	O at. %	N at. %	S at. %	K at. %	
180_KOH_W	56.6	30.1	12.4	0.2	0.0	0.8	
180_KOH_UW	43.4	33.1	21.2	0.1	0.1	2.1	
240_KOH_UW	46.2	31.5	20.0	0.1	0.0	2.3	
180_KOH_W_O3	54.8	37.5	7.5	0.2	0.1	0.0	
240_KOH_W_O3	56.2	32.1	11.6	0.2	0.0	0.0	
CO ₂ _2h	70.8	23.1	4.6	1.5	0.0	0.0	
K₂O		Elemental Analysis (EA)					
Element	C at. %	H at. %	O at. %	N at. %	S at. %	K at. %	
180_KOH_W	56.5	30.3	11.9	0.2	0.0	1.1	
180_KOH_UW	43.1	33.6	20.0	0.1	0.1	3.1	
240_KOH_UW	45.9	32.1	18.6	0.1	0.0	3.4	
180_KOH_W_O3	54.8	37.5	7.5	0.2	0.1	0.0	
240_KOH_W_O3	56.2	32.1	11.5	0.2	0.0	0.0	
CO ₂ _2h	70.8	23.1	4.6	1.5	0.0	0.0	
KHCO₃		Elemental Analysis (EA)					
Element	C at. %	H at. %	O at. %	N at. %	S at. %	K at. %	
180_KOH_W	56.2	30.4	12.7	0.2	0.0	0.5	
180_KOH_UW	42.8	33.7	21.9	0.1	0.1	1.4	
240_KOH_UW	45.4	32.2	20.7	0.1	0.0	1.5	
180_KOH_W_O3	54.8	37.5	7.5	0.2	0.1	0.0	
240_KOH_W_O3	56.2	32.1	11.6	0.2	0.0	0.0	
CO ₂ _2h	70.8	23.1	4.6	1.5	0.0	0.0	
KOOCH		Elemental Analysis (EA)					
Element	C at. %	H at. %	O at. %	N at. %	S at. %	K at. %	
180_KOH_W	56.3	30.5	12.4	0.2	0.0	0.6	
180_KOH_UW	43.1	34.0	21.1	0.1	0.1	1.7	
240_KOH_UW	45.7	32.5	19.8	0.1	0.0	1.8	
180_KOH_W_O3	54.8	37.5	7.5	0.2	0.1	0.0	
240_KOH_W_O3	56.2	32.1	11.6	0.2	0.0	0.0	
CO ₂ _2h	70.8	23.1	4.6	1.5	0.0	0.0	
K		Elemental Analysis (EA)					
Element	C at. %	H at. %	O at. %	N at. %	S at. %	K at. %	
180_KOH_W	56.7	30.4	11.4	0.2	0.0	1.4	
180_KOH_UW	43.5	33.9	18.6	0.1	0.1	3.8	
240_KOH_UW	46.3	32.4	17.1	0.1	0.0	4.1	
180_KOH_W_O3	54.8	37.5	7.5	0.2	0.1	0.0	
240_KOH_W_O3	56.2	32.1	11.5	0.2	0.0	0.0	
CO ₂ _2h	70.8	23.1	4.6	1.5	0.0	0.0	

Table S3: Position of XPS oxygen peaks in the O1s region, nature of the surface groups, and corresponding O content (at. %).

Materials	O1s			
	OI	OII	OIII	Oads*
Oxygen types	eV (at. %)	eV (at. %)	eV (at. %)	eV (at. %)
180_KOH_W	531.3 (19.4)	532.7 (45.6)	534.5 (15.3)	536.8 (19.7)
180_KOH_UW	531.5 (17.1)	532.7 (45.7)	534.6 (13.4)	536.5 (23.8)
240_KOH_UW	531.2 (25.7)	532.6 (41.5)	534.5 (16.2)	536.6 (16.6)
180_KOH_W_O3	531.5 (29.6)	532.7 (46.3)	534.5 (12.6)	536.9 (11.5)
240_KOH_W_O3	531.4 (23.6)	532.9 (49.1)	535.1 (6.9)	537.5 (20.4)
CO2_2h	531.2 (12.1)	532.8 (35.6)	535.1 (9.1)	537.4 (43.2)

OI : Carbonyl oxygen in quinones (531.0-531.9 eV)

OII: Carbonyl oxygen in esters, anhydrides and hydroxyls (532.3-532.8 eV) and non-carbonyl oxygen (ether-type) in esters and anhydrides (533.1-533.8 eV)

OIII: Oxygen in carboxyl groups (534.3-535.4 eV)

Oads*: Oxygen in adsorbed water or O₂ (536-536.5 eV)

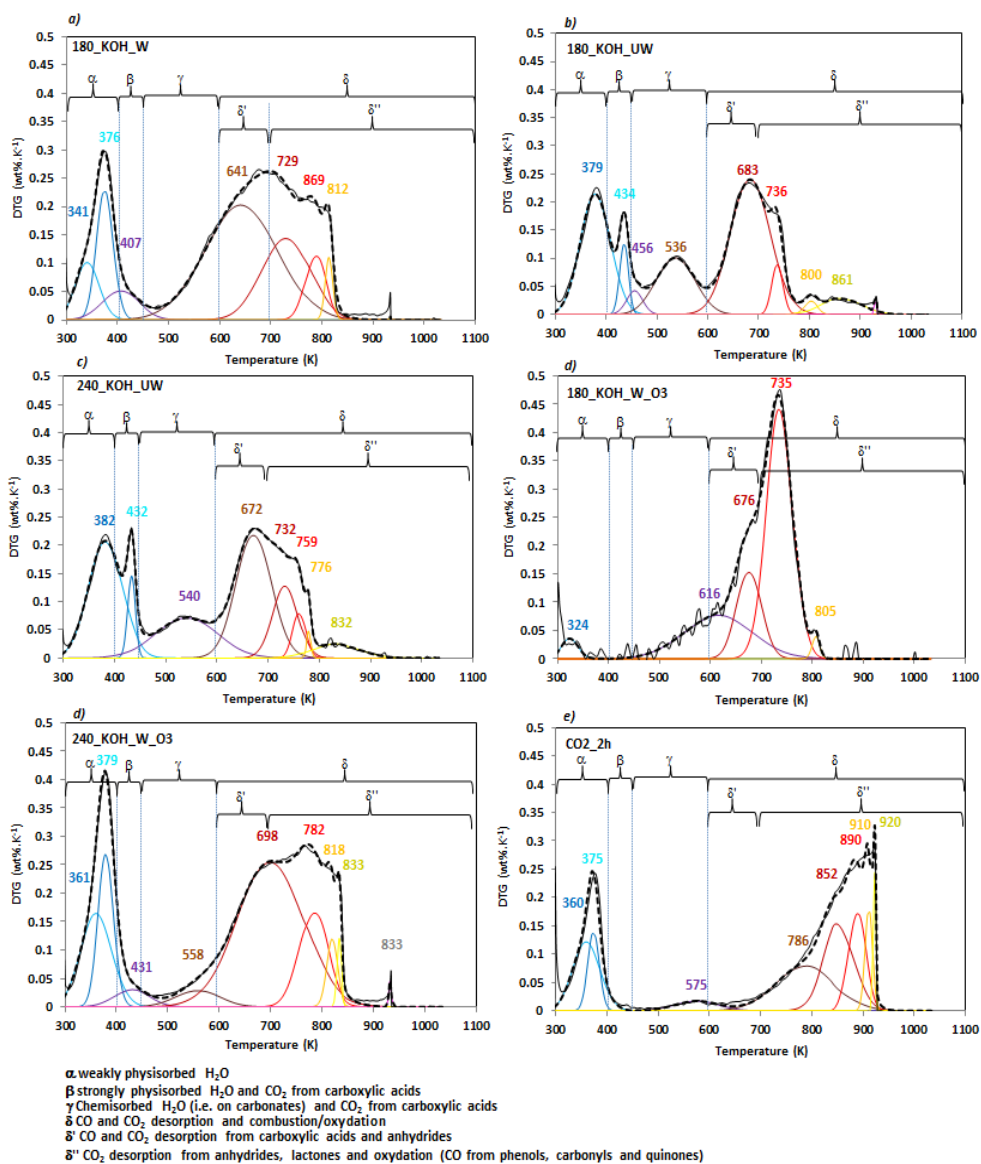


Figure S2: Reversed differential thermogravimetric curves of all carbon materials investigated here.

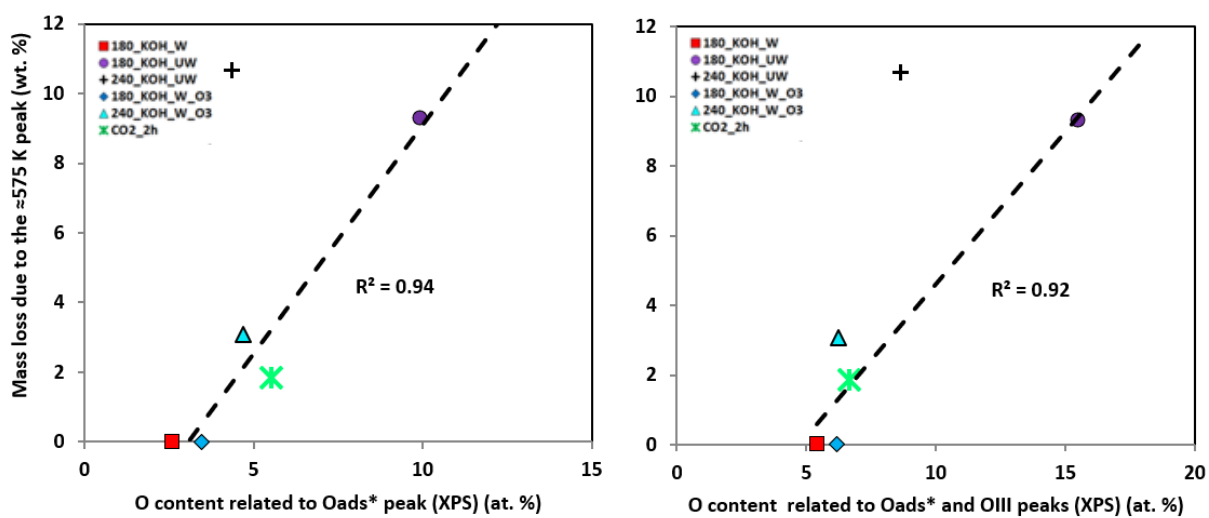


Figure S3: Correlation between the mass loss of the 540-575 K peak (DTG) and the O content in the surface functions related to **a)** Oads* and **b)** Oads* and OIII XPS peaks.

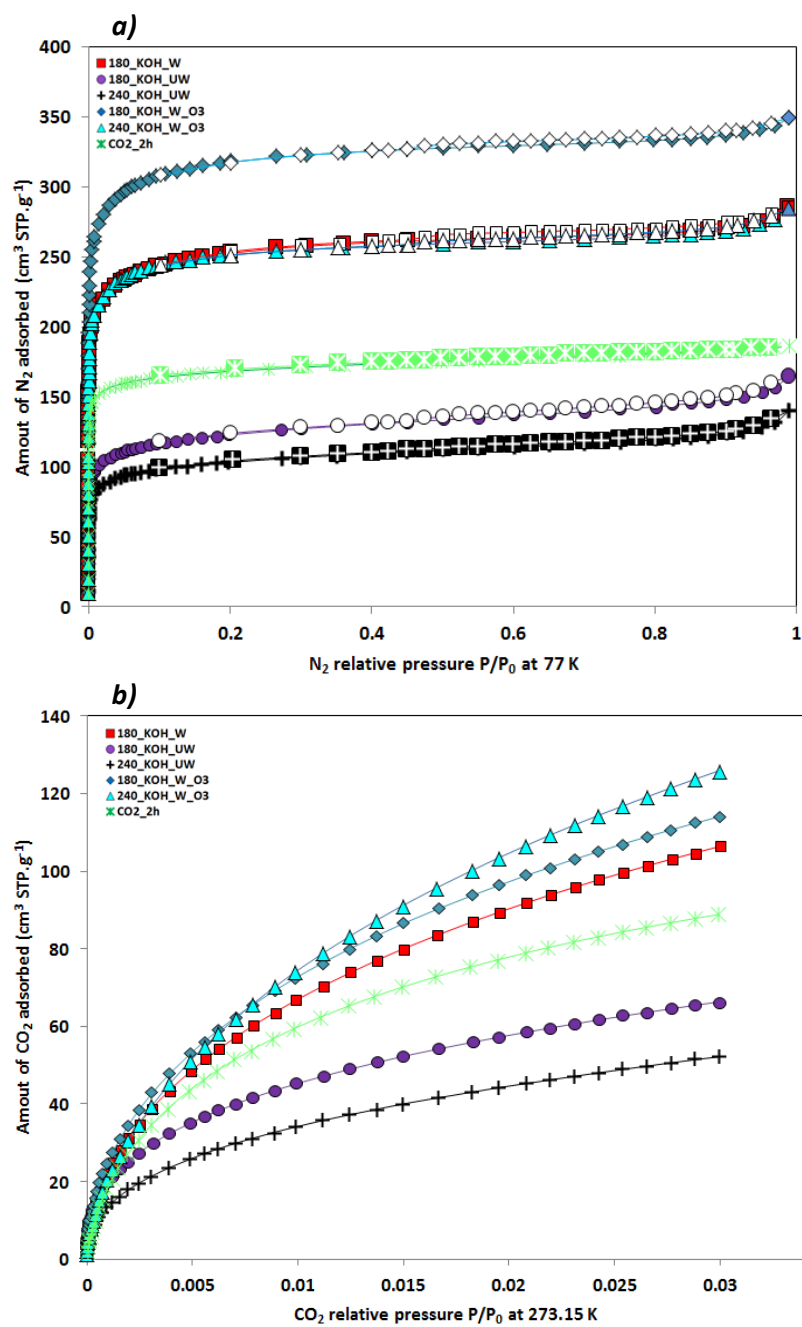


Figure S4: **a)** Nitrogen (77 K) and **b)** carbon dioxide (273 K) adsorption (closed symbols) and desorption (open symbols) isotherms of the materials.

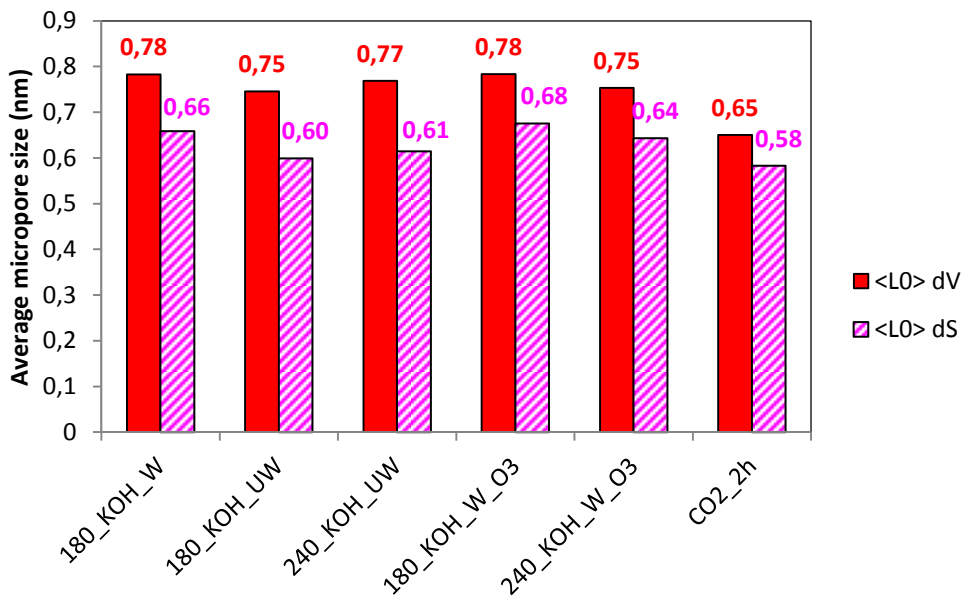


Figure S5: Average micropore sizes obtained using volume- ($\langle L_0 \rangle dV$) or surface-weighting ($\langle L_0 \rangle dS$) of the materials, according to the NLDFT.

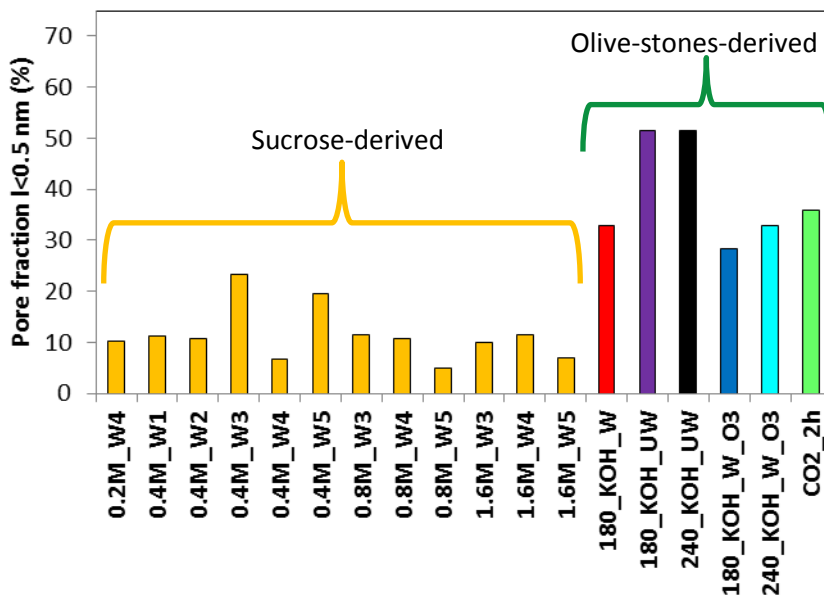


Figure S6: Fraction of micropores narrower than 0.5 nm in sucrose-derived ACs (data taken from [13]) and the olive-stone derived ACs and hybrid carbons.

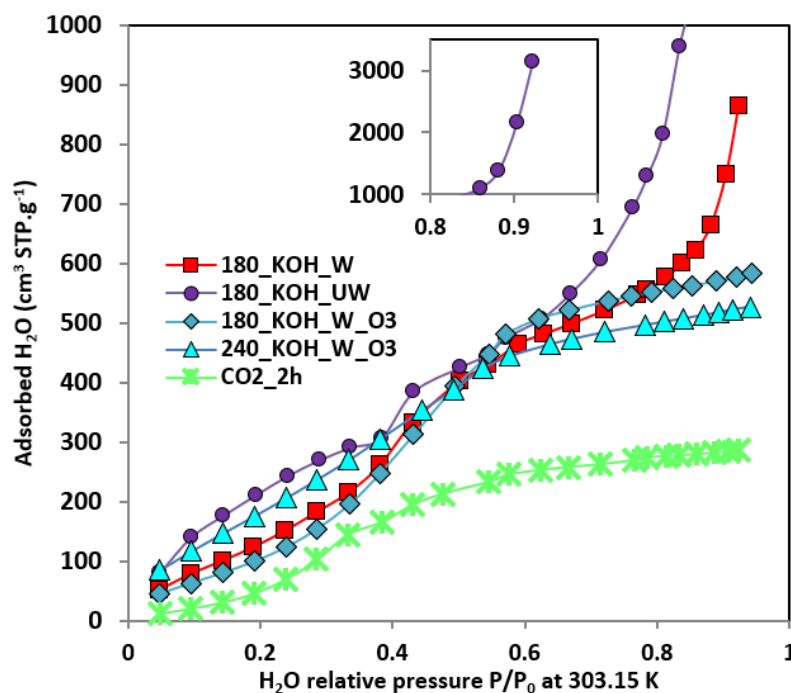


Figure S7: H₂O adsorption isotherms of the OS-derived materials (303.15 K).

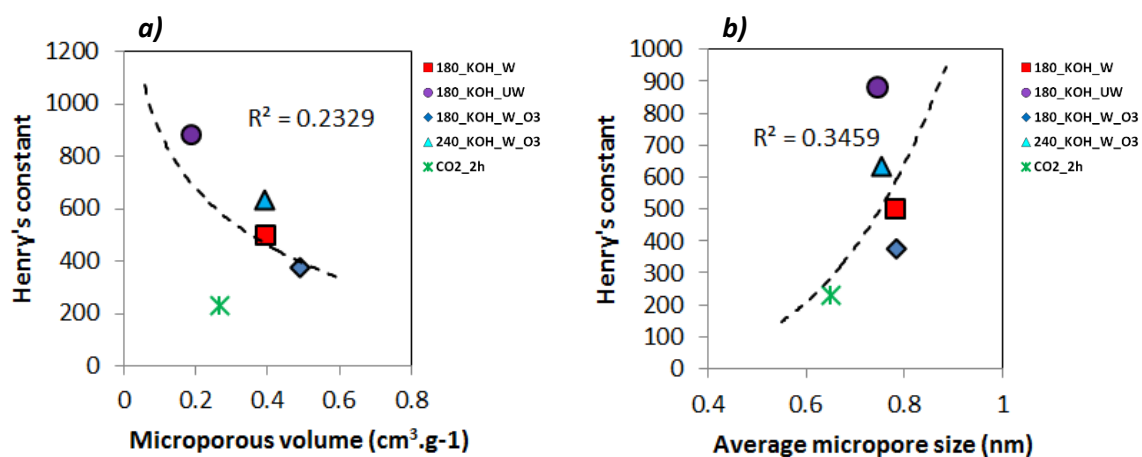


Figure S8: Dependence between Henry's constant, obtained from linear regressions of H₂O adsorption isotherms in the low-pressure range ($P/P_0 < 0.2$) on **a)** the microporous volume and **b)** the average micropore size.

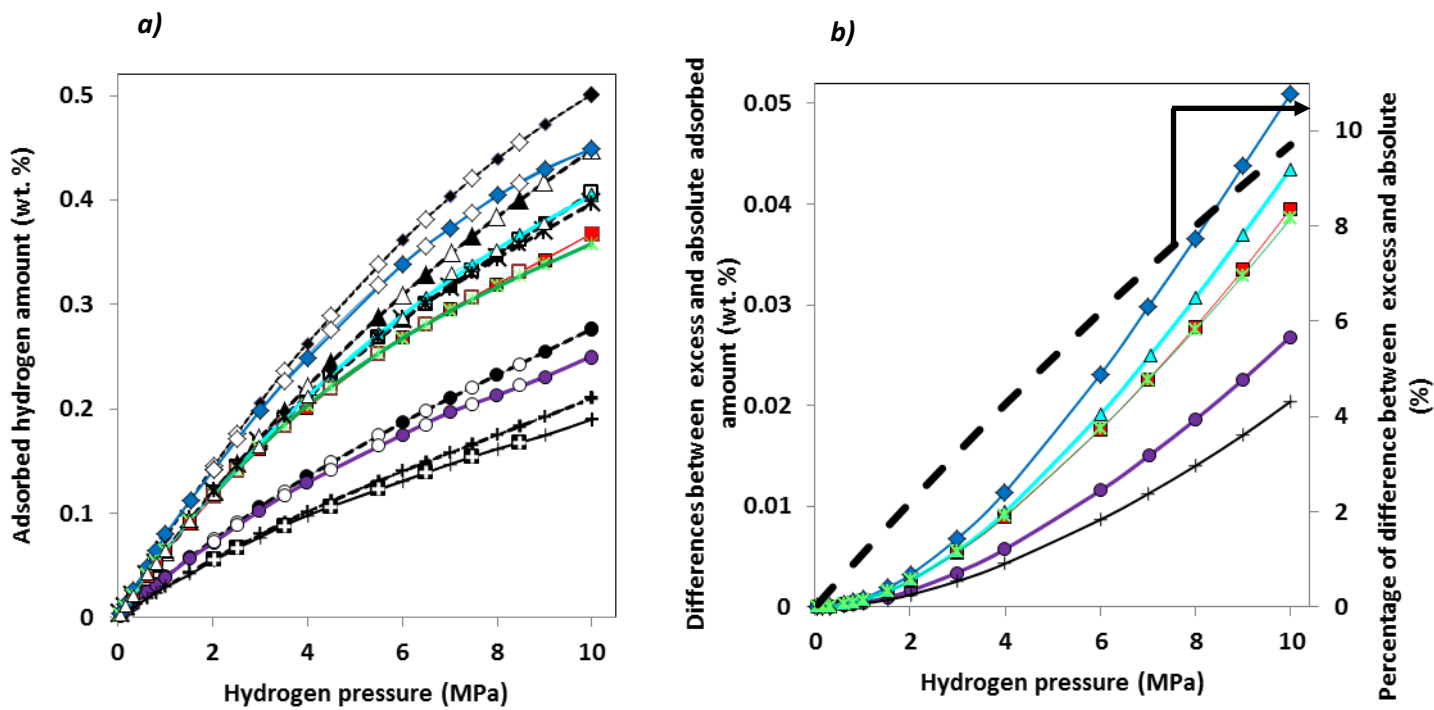


Figure S9: **a)** Excess (solid lines) and absolute (dashed lines) hydrogen adsorption (full symbols) – desorption (empty symbols) isotherms at 298.15 K, and **b)** difference between excess and absolute amounts as a function of pressure.

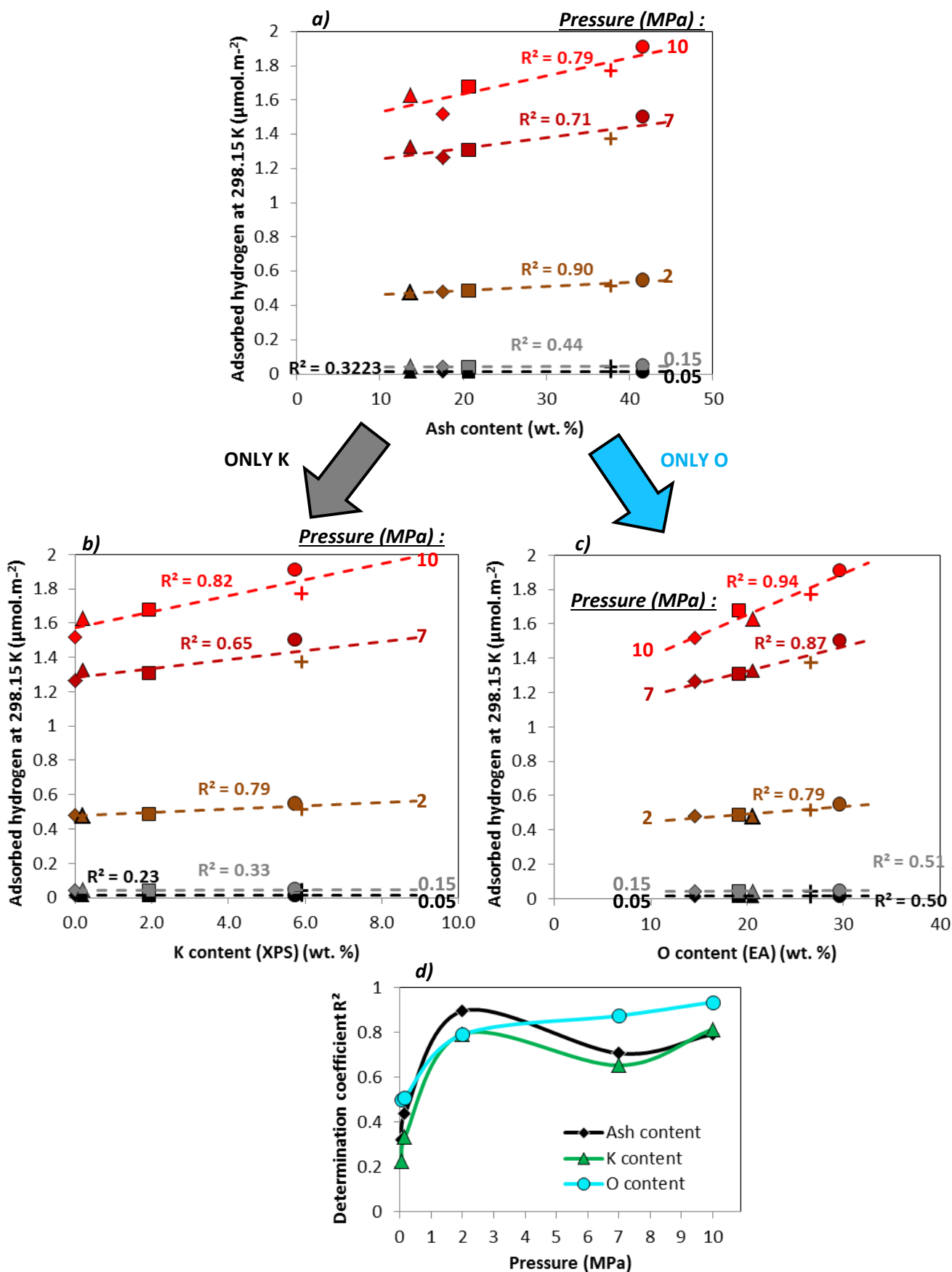


Figure S10: a) Correlation between absolute adsorbed amount per unit of surface area at 298.15 K and a) ash content, b) potassium content (XPS), and c) oxygen content (EA); d) determination coefficient of the different linear fits as a function of pressure.